Do Electrostatic Interactions Destabilize Protein–Nucleic Acid Binding?

Sanbo Qin,[1] Huan-Xiang Zhou[1,2]

[1] *Institute of Molecular Biophysics, School of Computational Science, Florida State University, Tallahassee, FL 32306*

[2] *Department of Physics, Florida State University, Tallahassee, FL 32306*

Received 5 January 2007; revised 13 February 2007; accepted 14 February 2007
Published online 26 February 2007 in Wiley InterScience (www.interscience.wiley.com). DOI 10.1002/bip.20708

ABSTRACT:

The negatively charged phosphates of nucleic acids are often paired with positively charged residues upon binding proteins. It was thus counter-intuitive when previous Poisson–Boltzmann (PB) calculations gave positive energies from electrostatic interactions, meaning that they destabilize protein–nucleic acid binding. Our own PB calculations on protein–protein binding have shown that the sign and the magnitude of the electrostatic component are sensitive to the specification of the dielectric boundary in PB calculations. A popular choice for the boundary between the solute low dielectric and the solvent high dielectric is the molecular surface; an alternative is the van der Waals (vdW) surface. In line with results for protein–protein binding, in this article, we found that PB calculations with the molecular surface gave positive electrostatic interaction energies for two protein–RNA complexes, but the signs are reversed when the vdW surface was used. Therefore, whether destabilizing or stabilizing effects are predicted depends on the choice of the dielectric boundary. The two calculation protocols, however, yielded similar salt effects on the binding affinity. Effects of charge mutations differentiated the two calculation protocols; PB calculations with the vdW surface had smaller deviations overall from experimental data. © *2007 Wiley Periodicals, Inc. Biopolymers 86: 112–118, 2007.*

Keywords: electrostatic interactions; DNA; RNA; salt effects; Poisson–Boltzmann equation

This article was originally published online as an accepted preprint. The "Published Online" date corresponds to the preprint version. You can request a copy of the preprint by emailing the Biopolymers editorial office at biopolymers@wiley.com

INTRODUCTION

The negative charges on the phosphates of DNA and RNA play dominant roles in their conformations and their interactions with proteins. Nucleic acid binding sites on proteins are known to be enriched in positively charged residues.[1,2] However, many calculations have found that electrostatic interaction energies between proteins and nucleic acids are positive, meaning that electrostatic interactions are destabilizing for their binding (see Table I).[3–13] These calculation results are very counter-intuitive. They were obtained from solving the Poisson–Boltzmann (PB) equation by choosing the molecular surface as the boundary between the solute low dielectric and the solvent dielectric. We have explored an alternative choice, i.e., the van der Waals (vdW) surface, and found that the electrostatic interaction energy is quite sensitive to the choice of the dielectric boundary.[14–17] In the case of protein–protein binding, the sign of the electrostatic interaction energies can be changed from positive to negative when the choice of dielectric boundary is changed from the molecular surface to the vdW surface.[16,17] In this article, we study the effect of the dielectric boundary on the electrostatic interaction energies of two protein–RNA complexes, and re-examine the previous conclusion that electrostatic interactions destabilize protein–nucleic acid binding.

Correspondence to: Huan-Xiang Zhou; e-mail: zhou@sb.fsu.edu
Contract grant sponsor: NIH
Contract grant number: GM058187

Table I Electrostatic Contributions to Binding Stability of Protein–Nucleic Acid Complexes Calculated in Previous Studies

Protein:Nucleic Acid Complex	ΔG_{el}(kcal/mol)	$I(M)$	$(\varepsilon_i,\varepsilon_s)$	PB Solver	Authors (year)
λ repressor:operator	−7	0.122	(2, 78)	UHBD	Zacharias et al. (1992)[3]
Homeodomains:DNA	−23.9 to 38.2	0.145	(2, 78)	UHBD	Fogolari et al. (1997)[4]
λcI repressor:DNA	73	0.2	(2, 80)	DelPhi	Misra et al. (1998)[5]
434 repressor: and cro:DNA	19.1 and 5.7	0.1	(4, 78)	CONGEN	Brown et al. (1998)[6]
Ricin A chain:rRNA	68.6/19.3	0.145	(2/7, 80)	DelPhi	Olson and Cuff (1999)[7]
U1A:RNA	85	0.15	(1, 80)	DelPhi	Reyes and Kollman (2000)[8]
U1A:RNA	22.7	0.145	(4, 80)	DelPhi	Olson (2001)[9]
Tn916:DNA	8	0.15	(1, 80)	DelPhi	Gorfe and Jelesarov (2003)[10]
20 protein:DNA complexes	11 avg. 47; 9 avg. −22	0.145	(2, 80)	DelPhi	Norberg (2003)[11]
Telomere end binding protein:DNA	13.1	0.15	(4, 80)	UHBD	Wojciechowski et al. (2005)[12]
TATA-box binding protein:TATA box	72	0.13	(1, 80)	DelPhi	Zhang and Schlick (2006)[13]

The two protein–RNA complexes studied here are formed by the A protein of the U1 small nuclear ribonucleoprotein particle and its stem-loop RNA target (U1hpII), and by the C-terminal domain of ribosomal protein L11 (L11-C76) and a 58-nucleotide domain of 23 S rRNA (see Figure 1). The structures of these complexes have been determined by X-ray diffraction.[18,19] The effects of salts and charge mutations on their binding stability have also been measured.[20–22] The U1A:U1hpII complex has served as a model system for previous theoretical studies.[8,9]

We calculated the electrostatic interaction energies from the nonlinear PB equation using two popular programs: UHBD[23] and Delphi.[24,25] The dielectric boundary was set to either the vdW surface or the molecular surface; the latter excludes a 1.4-Å solvent probe from the solute interior. For specificity, the latter is referred to as the solvent-exclusion (SE) surface in the paper. The difference between the two surfaces lies in the numerous small crevices which cannot be accessed by the solvent probe. These crevices are assigned as part of the solvent dielectric in the vdW specification, but as part of the solute dielectric in the SE specification. The overall electrostatic interaction energy between two subunits in a complex is determined by the balance of two opposing contributions: the unfavorable desolvation cost of the charges on the subunits and the favorable interactions between the charges across the interface. Relative to the vdW specification, the SE specification gives rise to higher desolvation cost for charges and stronger interactions between charges. This tilts the balance of the two contributions, leading to the change from electrostatic stabilization to electrostatic destabilization found in protein–protein binding.[16,17] Here again we found that electrostatic interaction energies for the two protein–RNA complexes were positive when the dielectric boundary was chosen as the SE surface but became negative when the vdW surface was used.

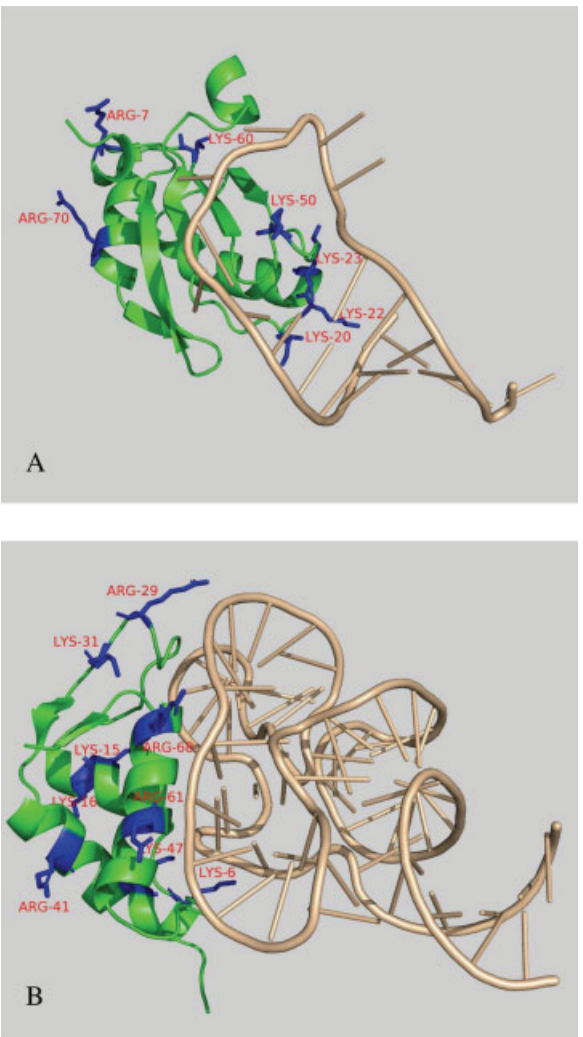

FIGURE 1 Structures of two protein–RNA complexes studied. (A) U1A:U1hpII. (B) L11-C76:rRNA. Side chains of mutated residues are shown. Pictures were generated by PyMOL (http://www.pymol.org) using PDB entries 1urn and 1hc8.

In previous studies, it has been found that calculated salt effects are insensitive to the details of charge distribution[3] and to the choice of the dielectric boundary.[16,26] In line with these studies, the salt effects calculated on the two protein–RNA complexes were found to be very similar when either vdW or SE was chosen as the dielectric boundary, and were in reasonable agreement with experimental data. Thus unfortunately experimental salt effects cannot be used to discriminate between the two choices of the dielectric boundary. However, effects of charge mutations calculated with the two choices of dielectric boundary were different. Consistent with a series of previous studies,[14–17] the vdW calculations gave better agreement with experimental data.

METHODS

Electrostatic Contribution to Protein–RNA Binding

The contribution of electrostatic interactions between a protein and an RNA to the binding free energy was calculated as

$$\Delta G_{el} = G_{el}(\text{protein–RNA}) - G_{el}(\text{protein}) - G_{el}(\text{RNA}) \quad (1)$$

where G_{el} is the total electrostatic energy of a solute molecule, which is the work of charging up the solute molecule in both the linearized and nonlinear PB equations.[27] A negative value for ΔG_{el} indicates that electrostatic interactions are stabilizing for protein–RNA binding.

The effects of salt concentration and charge mutations on ΔG_{el} were compared with experimental data. Throughout the article, we use $\Delta\Delta G_{el} = \Delta G_{el}(\text{mut}) - \Delta G_{el}(\text{WT})$ to denote the change in ΔG_{el} from the wild-type protein to a mutant, and $\delta\Delta G_{el} = \Delta G_{el}(I) - \Delta G_{el}(I_0)$ to denote the change in ΔG_{el} from salt concentration I_0 to I. The experimental counterpart of $\Delta\Delta G_{el}$ is $-k_B T \ln[K_a(\text{mut})/K_a(\text{WT})]$, where k_B is the Boltzmann constant, T is absolute temperature, and $K_a(\text{mut})$ and $K_a(\text{WT})$ are the measured RNA-binding equilibrium constants of the mutant and wild-type proteins, respectively. Similarly, the experimental quantity corresponding to $\delta\Delta G_{el}$ is $-k_B T \ln[K_a(I)/K_a(I_0)]$. Salt effects were also assessed by $\partial\Delta G_{el}/k_B T \partial \ln I$ and its experimental counterpart $-\partial \log K_a/\partial \log I$.

Solution of the Nonlinear Poisson–Boltzmann Equation

The UHBD program was used as in previous studies.[14–17] Briefly, the calculation began with a coarse grid with a 1.5 Å spacing, and then a finer grid with a 0.5 Å spacing, both centered at the geometric center of the solute molecule. A final grid with a 0.25 Å spacing was centered at the site of mutation. The dimensions of all the three grids were 140 Å × 140 Å × 140 Å. To reduce errors caused by distributing solute charges to the grids, the nonlinear PB equation was solved twice, once with the solvent variables (i.e., solvent dielectric constant ε_s and ionic strength I) set to the intended values and once with their values set to the solute dielectric constant ε_i and 0, respectively. The ion exclusion radius in the first calculation was 2 Å. The total electrostatic energy G_{el} was the sum of the solvation energy, obtained as the difference between the two calculations, and the Coulomb term, calculated according to Coulomb's law with a dielectric constant ε_i. The difference between a vdW and an SE calculation was an extra option "nmap 1.4, nsph 500" in the input script for the latter.

The protocol for DelPhi calculations was similar. A coarse grid with a 1.5-Å spacing was followed by a grid with a 0.5-Å spacing, with Cartesian coordinates of their center at midpoints of extreme values of atomic coordinates of the wild-type complex. The dimensions of the two grids were 257 Å × 257 Å × 257 Å. vdW and SE was selected by setting PROBERADIUS to 0 and 1.4, respectively, in the parameter file.

For maximum error cancellation, the atomic positions and charges were identical in the bound and unbound states. When calculating effects of salts or mutations, the grid centers of all related calculations were made sure to be identical.

Molecular Structures and Parameters

The U1A:U1hpII complex was based on the B and Q chains of the X-ray structure of human U1A complexed with RNA hairpin 5′-AAUCCAUUGCACUCCGGAUUU-3′ (Protein Data Bank entry 1urn).[18] To better match the RNA used in the experimental studies: 5′-AGCUUAUAUCCAUUGCACUCCGGAUGAGCU-3′,[20,21] the 5′ adenine and two 3′ uracils in 1urn were removed and a 5 basepair duplex RNA (5′-AGCUU paired with AAGCU-3′) was added in InsightII (Accelrys Software, San Diego). Two mutations in 1urn, His31, and ARG36, were mutated back to the wild-type residues, Tyr31 and Gln36, respectively. Finally hydrogens were added and the complex was energy minimized with Amber 9.[28] For compatibility with the Amber force field, the phosphate at the 5′-end of U1hpII was removed; the net charge on the RNA was $-27e$. The protein had a net charge of $+6e$. For the L11-C76:rRNA complex, chains A and C of PDB entry 1hc8 were used. An internal K^+ was retained as part of the RNA. With removal of the 5′-end phosphate, the net charge of the 58-nucleotide RNA was $-56e$ for the RNA. The net charge on the protein was $+3e$.

Mutations were modeled in InsightII and then energy-minimized with Amber 9.[28] Only mutated side chains were allowed to move during minimization; otherwise the energetic contribution of the mutation would be overwhelmed, in a single-conformation calculation, by those from changes in other parts of the molecule. Because of concerns for potential inadequacy in the modeling of mutations, our study was restricted to single mutations, except for one double mutation (K20A/K22A) on the U1A:U1hpII complex.

In all electrostatic calculations, protein atoms were assigned AMBER charges[29] and Bondi radii.[30] The temperature was set to 298 K, and the solute and solvent dielectric constants were 4 and 78.5, respectively. The buffer for the experimental studies on the U1A:U1hpII complex was 10 m*M* Tris-HCl and 150 m*M* (or a higher concentration) NaCl.[20,21] This was modeled with an ionic strength of 160 m*M* (or higher). The buffer for the experimental studies on the L11-C76:rRNA complex was 10 m*M* Mops, 3 m*M* $MgCl_2$, and 175 m*M* (or a higher concentration) KCl.[22] We modeled this buffer either with an ionic strength (or 1:1 salt) of 194 m*M* (or higher) or as a mixture of 185 m*M* 1:1 salt and 3 m*M* $MgCl_2$. Calculations with the DelPhi program found the results to be very similar. All results reported below were from modeling the buffer as a single 1:1 salt.

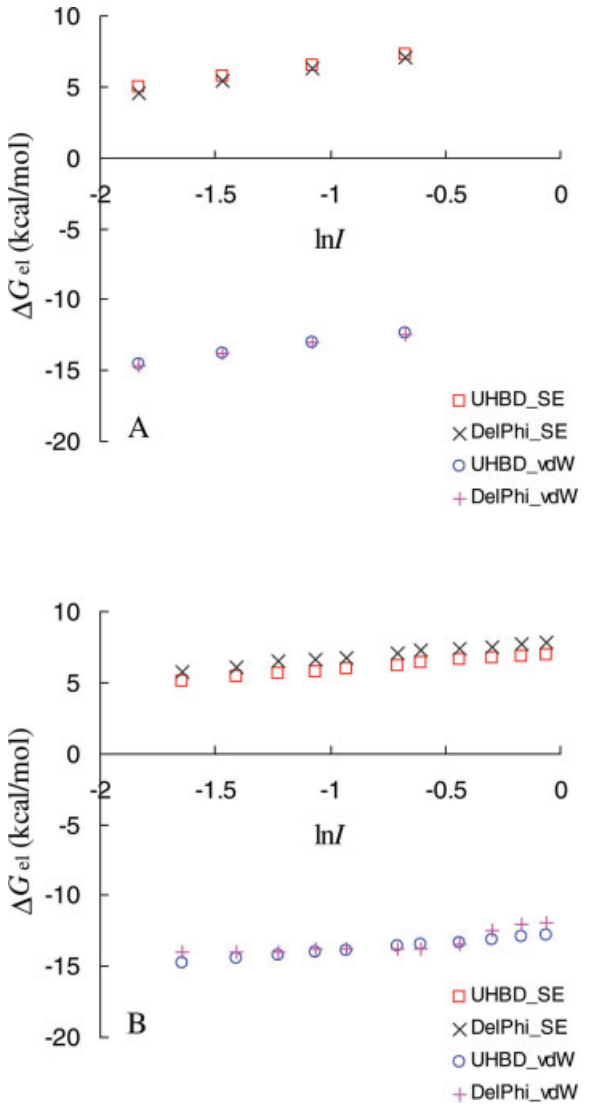

FIGURE 2 Overall electrostatic contributions to protein–RNA binding. (A) U1A:U1hpII. (B) L11-C76:rRNA. Results calculated from both the UHBD and the DelPhi programs, with the dielectric boundary set to either vdW or SE, are shown. UHBD calculations involved a second focusing, on a site of mutation; results shown are the averages over seven focusing sites for U1A:U1hpII and over nine focusing sites for L11-C76:rRNA.

RESULTS AND DISCUSSION

Overall Electrostatic Contribution to Protein–RNA Binding

In Figure 2, we present the results of ΔG_{el} for the U1A:U1hpII and L11-C76:rRNA complexes at different ionic strengths, calculated with the dielectric boundary set either to vdW or SE. The UHBD and DelPhi programs gave very similar values. For U1A:U1hpII, the SE results varied from 5.0 to 7.2 kcal/mol when I increased from 160 to 510 mM. In contrast, the vdW results varied from −14.6 to −12.4 kcal/mol over this range of salt concentration. ΔG_{el} for L11-C76:rRNA also changed from positive to negative when the dielectric boundary was set to the vdW surface instead of the SE surface. The SE and vdW results varied from 5.1 to 7.0 kcal/mol and from −14.8 to −12.8 kcal/mol, respectively, when I increased from 194 to 944 mM.

The SE results indicate that electrostatic interactions become more and more destabilizing as salt concentration is increased. On the other hand, the vdW results indicate that electrostatic interactions become less and less stabilizing as salt concentration is increased. The latter trend is consistent with the intuitive notion that salts screen out favorable interactions between two oppositely charged molecules.

These results of ΔG_{el} were calculated with a protein dielectric constant of 4. To explore the effect of the protein dielectric constant, we also calculated ΔG_{el} for U1A:U1hpII at $I =$ 160 mM with ε_i at 1, 2, and 8 by the UHBD program. The vdW results were −33.6, −20.8, and −11.6 kcal/mol, respectively. These have the same sign as the $\varepsilon_i = 4$ result, but with diminishing magnitudes as ε_i increases. The SE results at $\varepsilon_i =$ 1, 2, and 8 were 48.9, 19.7, and −2.5 kcal/mol, respectively. The sign switch at $\varepsilon_i = 8$ is a reflection of reduced desolvation cost, obtained when a high protein dielectric constant is used. An artificially high protein dielectric constant has been proposed to fix the problem of excessive shifts in pK_a predictions.[31]

Salt Effects on ΔG_{el} of Wild Type and Mutant Complexes

While the signs of ΔG_{el} calculated with the SE and vdW protocols are opposite, very similar changes in ΔG_{el} over a range of salt concentration were obtained. Figure 3A shows the changes in ΔG_{el} from $I =$ 160 to 230, 340, and 510 mM for the U1A:U1hpII complex. Reasonable agreement with the experimental results of Law et al.[21] can be seen.

In Figure 3B, we compare the slopes of linear fits to the dependence of $\Delta G_{el}/k_BT$ on ln$I$, with the experimental counterparts[22] for wild-type and nine mutant L11-C76:rRNA complexes. The nine mutations were: K6A, K15A, K16A, R29A, K31A, R41A, K47M, R61A, and R68A (see Figure 1B). Relative to the experimental results, the magnitudes of the slopes were overestimated by the PB calculations. Nevertheless the rank order among the 10 complexes appeared to be predicted well. According to both experiment and calculation, WT, K16A, K31A, and R41A had higher slopes than K6A, K15A, R61A, and R68A. The latter mutated residues are much closer to the protein–RNA interface than the former ones are to the interface (see Figure 1B), hence the

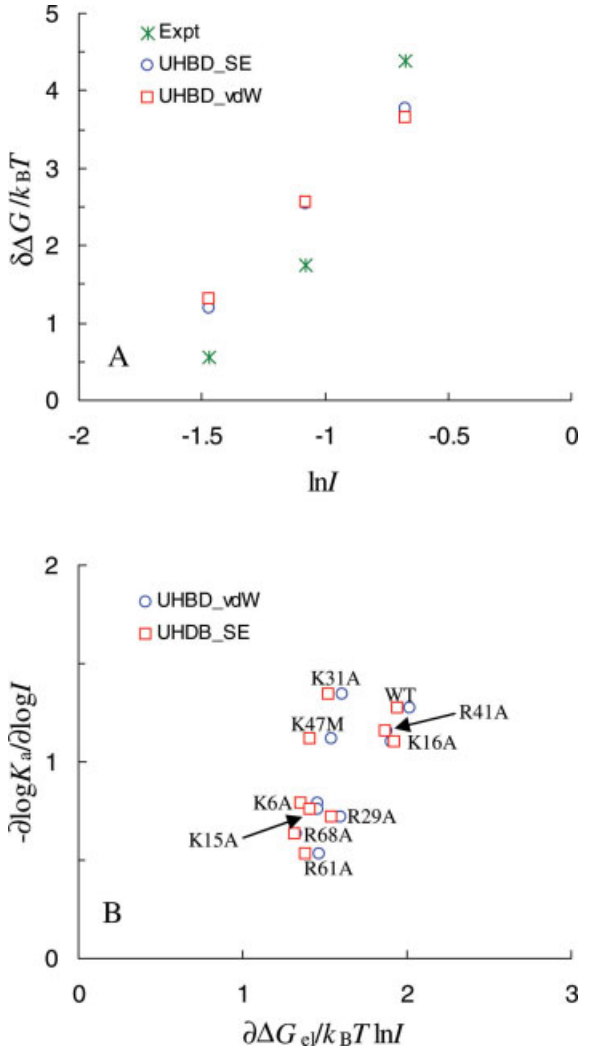

FIGURE 3 Comparison of calculated and experimental results for salt effects on the binding energy. (A) U1A:U1hpII. (B) L11-C76:rRNA. In panel (B), each data point represents a pair of calculated (abscissa) and experimental (ordinate) values for either the wild-type complex or one of the nine mutants. Though only UHBD results are shown, results obtained by the DelPhi program were very similar.

mutations would be expected to have a larger impact on the salt slope of the wild-type complex.

Effects of Charge Mutations

For the U1A:U1hpII complex, we studied the effects of seven single mutations, R7Q, K20Q, K22Q, K23Q, K50A, K60Q, and R70Q, and one double mutant, K20A/K22A, on ΔG_{el} at I = 160 mM. Figure 4A shows the comparison of $\Delta\Delta G_{el}$, calculated by both the vdW and SE protocols, with the experimental data,[20,21] assuming that the effects of mutations are dominated by electrostatic contributions (see later). The significantly larger effects of the K20Q, K22Q, K20A/K22A, K23Q, and K50A mutations over those of the R7Q, K60Q, and R70Q mutations can be rationalized by the much smaller distances of the former residues from the protein–RNA interface (see Figure 1A).

The root-mean-square-deviation (RMSD) of the vdW results from the experimental data was 0.4 kcal/mol. The RMSD for the SE results was substantially higher, at 1.0 kcal/mol. The K22Q mutation was incorrectly predicted by the SE protocol to be stabilizing, indicating that the desolvation cost for K22 in the wild-type complex was overestimated. In addition, the destabilizing effect of the K20A/K22A mutation was substantially underestimated by the SE protocol.

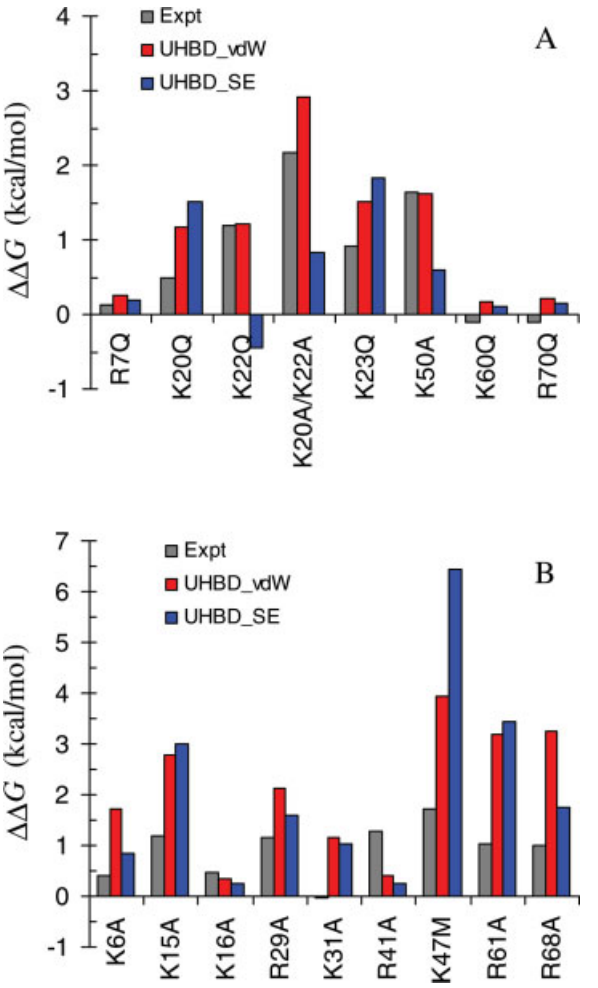

FIGURE 4 Comparison of calculated and experimental results for the effects of mutations on the binding energy. (A) U1A:U1hpII. (B) L11-C76:rRNA. The ionic strengths for the two complexes were 160 and 194 mM, respectively. UHBD results are shown. Very similar results were obtained by the DelPhi program, with RMSD between UHBD and DelPhi results at 0.2 kcal/mol among the eight U1A:U1hpII mutations and at 0.1 kcal/mol among the nine L11-C76:rRNA mutations.

Comparison between calculated $\Delta\Delta G_{el}$ and the experimental counterparts[22] at $I = 194$ mM for the nine mutations on the L11-C76:rRNA complex is shown in Figure 4B. Again, the RMSD from experimental data was smaller for the vdW calculations (at 1.6 kcal/mol) than for the SE calculations (at 2.0 kcal/mol). The latter calculations significantly overestimated the effect of the K47M mutation.

Choice Between vdW and SE

Our calculations found very similar salt effects between the vdW and SE protocols, in agreement with results obtained previously on a protein–protein complex.[16] Good predictions of salt effects provided much support for the PB approach to modeling electrostatic interactions in protein–nucleic acid complexes.[32] However, since very similar salt effects are predicted by the vdW and SE protocols, experimental data on salt effects unfortunately cannot be used to discriminate between the two choices of the dielectric boundary.

Effects of charge mutations are predicted differently by the two protocols. Better agreement with experiment was obtained by the vdW calculations for both of the protein–RNA complexes studied here. This adds to a large body of data for the effects of charge mutations on protein folding and binding stability that points to the same conclusion.[14–17,33,34]

A caveat on mutational data is that electrostatic interactions are assumed to make dominant contributions to the effects of mutation. Experiments measure the total effects of mutations, which may have both electrostatic and nonelectrostatic contributions, but PB calculations only give the electrostatic contributions. One way out of this conundrum is to use experimental data for mutational effects on the binding rate instead of the binding affinity. In the translent complex formed by transitional and rotational diffusion, the two subunits are solvent separated and thus there electrostatic interactions indeed provide the dominant contributions.[35–37] A characteristic of electrostatically enhanced diffusion-limited protein association is that ionic strength show disparate effects on the on and off rates, significant on the former but modest on the latter.[38,39] The on and off rates of the U1A:U1hpII complex measured by Laird-Offringa and coworkers[20,21] follow exactly this characteristic. The data on the on rates will thus enable further discrimination of the vdW and SE protocols. Such a study is underway.

Do Electrostatic Interactions Destabilize Protein–Nucleic Acid Binding?

Our results on the two protein–RNA complexes show that whether or not electrostatic interactions are predicted to be stabilizing or destabilizing for binding depends on the choice of the dielectric boundary in PB calculations, in line with previous studies on protein–protein complexes.[16,17,33] SE calculations lead to destabilization whereas vdW calculations lead to stabilization. This finding suggests that the conclusion of electrostatic destabilization, previously reached from PB calculations with the SE dielectric boundary, is open to question.

The SE specification is based on a static structure for the solute molecule and a 1.4-Å spherical model for the solvent water molecule. Hydrogen experiments demonstrate that, due to the dynamic nature of proteins, the interior is highly accessible to solvent; NMR experiments have shown the occupancy of water in internal cavities.[40] Molecular dynamics simulations have also shown that water molecules can penetrate into the protein interior[41] and that the hydrogen and oxygen atoms of a water molecule can penetrate the vdW surface of an ion.[42] These results suggest that the crevices outside atomic vdW spheres are accessible to solvent, as modeled by the vdW specification.

We do not yet have a definitive answer to the very basic question of whether electrostatic interactions are stabilizing or destabilizing for protein–nucleic acid binding. However, there is accumulating evidence pointing toward the stabilizing answer.

REFERENCES

1. Luscombe, N. M.; Laskowski, R. A.; Thornton, J. M. Nucleic Acids Res 2001, 29, 2860–2874.
2. Tjong, H.; Zhou, H.-X. Nucleic Acids Res, in press.
3. Zacharias, M.; Luty, B. A.; Davis, M. E.; McCammon, J. A. Biophys J 1992, 63, 1280–1285.
4. Fogolari, F.; Elcock, A. H.; Esposito, G.; Viglino, P.; Briggs, J. M.; McCammon, J. A. J Mol Biol 1997, 267, 368–381.
5. Misra, V. K.; Hecht, J. L.; Yang, A. S.; Honig, B. Biophys J 1998, 75, 2262–2273.
6. Brown, L. M.; Bruccoleri, R. E.; Novotny, J. Pac Symp Biocomput 1998, 339–348.
7. Olson, M. A.; Cuff, L. Biophys J 1999, 76, 28–39.
8. Reyes, C. M.; Kollman, P. A. J Mol Biol 2000, 297, 1145–1158.
9. Olson, M. A. Biophys J 2001, 81, 1841–1853.
10. Gorfe, A. A.; Jelesarov, I. Biochemistry 2003, 42, 11568–11576.
11. Norberg, J. Arch Biochem Biophys 2003, 410, 48–68.
12. Wojciechowski, M.; Fogolari, F.; Baginski, M. J Struct Biol 2005, 152, 169–184.
13. Zhang, Q.; Schlick, T. Biophys J 2006, 90, 1865–1877.
14. Vijayakumar, M.; Zhou, H.-X. J Phys Chem B 2001, 101, 7334–7340.
15. Dong, F.; Zhou, H.-X. Biophys J 2002, 83, 1341–1347.
16. Dong, F.; Vijayakumar, M.; Zhou, H.–X. Biophys J 2003, 85, 49–60.
17. Dong, F.; Zhou, H.-X. Proteins 2006, 65, 87–102.
18. Oubridge, C.; Ito, N.; Evans, P. R.; Teo, C. H.; Nagai, K. Nature 1994, 372, 432–438.

19. Conn, G. L.; Gittis, A. G.; Lattman, E. E.; Misra, V. K.; Draper, D. E. J Mol Biol 2002, 318, 963–973.
20. Katsamba, P. S.; Myszka, D. G.; Laird-Offringa, I. A. J Biol Chem 2001, 276, 21476–21481.
21. Law, M. J.; Linde, M. E.; Chambers, E. J.; Oubridge, C.; Katsamba, P. S.; Nilsson, L.; Haworth, I. S.; Laird-Offringa, I. A. Nucleic Acids Res 2006, 34, 275–285.
22. GuhaThakurta, D.; Draper, D. E. J Mol Biol 2000, 295, 569–580.
23. Madura, J. D.; Briggs, J. M.; Wade, R. C.; Davis, M. E.; Luty, B. A.; Ilin, A.; Antosiewicz, J.; Gilson, M. K.; Bagheri, B.; Scott, L. R.; McCammon, J. A. Comput Phys Comm 1995, 91, 57–95.
24. Gilson, M. K.; Honig, B. Proteins 1988, 4, 7–18.
25. Nicholls, A.; Honig, B. J Comput Chem 1991, 12, 435–445.
26. Tjong, H.; Zhou, H.-X. J Phys Chem B 2007, 111, 3055–3061.
27. Zhou, H.-X. J Chem Phys 1994, 100, 3152–3162.
28. Case, D. A.; Darden, T. A.; Cheatham, T. E. III; Simmerling, C. L.; Wang, J.; Duke, R. E.; Luo, R.; Merz, K. M.; Pearlman, D. A.; Crowley, M.; Walker, R. C.; Zhang, W.; Wang, B.; Hayik, S.; Roitberg, A.; Seabra, G.; Wong, K. F.; Paesani, F.; Wu, X.; Brozell, S.; Tsui, V.; Gohlke, H.; Yang, L.; Tan, C.; Mongan, J.; Hornak, V.; Cui, G.; Beroza, P.; Mathews, D. H.; Schafmeister, C.; Ross, W. S.; Kollman, P. A. Amber 9; University of California: San Francisco, CA, 2006.
29. Cornell, W. D.; Cieplak, P.; Bayly, C. I.; Gould, I. R.; Merz, K. M.; Ferguson, D. M.; Spellmeyer, D. C.; Fox, T.; Caldwell, J. W.; Kollman, P. A.J Am Chem Soc 1995, 117, 5179–5197.
30. Bondi, A. J Phys Chem 1964, 68, 441–451.
31. Antosiewicz, J.; McCammon, J. A.; Gilson, M. K. J Mol Biol 1994, 238, 415–436.
32. Misra, V. K.; Hecht, J. L.; Sharp, K. A.; Friedman, R. A.; Honig, B. J Mol Biol 1994, 238, 264–280.
33. Wang, T.; Tomic, S.; Gabdoulline, R. R.; Wade, R. C. Biophys J 2004, 87, 1618–1630.
34. De Rienzo, F.; Gabdoulline, R. R.; Menziani, M. C.; De Benedetti, P. G.; Wade, R. C. Biophys J 2001, 81, 3090–3104.
35. Vijayakumar, M.; Wong, K.-Y.; Schreiber, G.; Fersht, A. R.; Szabo, A.; Zhou, H.-X. J Mol Biol 1998, 278, 1015–1024.
36. Alsallaq, R.; Zhou, H.-X. Biophys J 2007, 92, 1486–1502.
37. Alsallaq, R.; Zhou, H.-X. Structure 2007, 15, 215–224.
38. Zhou, H.-X. Biopolymers 2001, 59, 427–433.
39. Zhou, H.-X. Protein Sci 2003, 12, 2379–2382.
40. Ernst, J. A.; Clubb, R. T.; Zhou, H. X.; Gronenborn, A. M.; Clore, G. M. Science 1995, 267, 1813–1817.
41. Damjanovic, A.; Garcia-Moreno, B.; Lattman, E. E.; Garcia, A. E. Proteins 2005, 60, 433–449.
42. Hummer, G.; Pratt, L. R.; Garcia, A. E. J Phys Chem 1996, 100, 1206–1215.

Reviewing Editor: Sarah Woodson